ISSN 2689-8268 | Volume 7

American Journal of Surgery and Clinical Case Reports

Case Report Open Access

Ewing Sarcoma of the Lumbar Spine With Lung Metastases in A 20-Year-Old Adult: A Rare Case Report

Balodis A[1,2], Eglīte E[4], Zarembo Z[1,2], Raits U[1], Dolgopolova J[3], Kalnina M[1] and Lapse D[5]

[1]Institute of Diagnostic Radiology, Pauls Stradins Clinical University Hospital, Riga, Latvia

[2]Department of Radiology, Riga Stradins University, Riga, Latvia

[3]Department of Neurosurgery, Pauls Stradins Clinical University Hospital, Riga, Latvia

[4]Riga Stradins University, Faculty of Medicine

[5]Department of Pathology, Riga Stradins University Hospital, Riga, Latvia

***Corresponding author:**

Arturs Balodis,
Institute of Diagnostic Radiology, Pauls Stradins Clinical University Hospital, Riga, Latvia

Received: 14 Jan 2024
Accepted: 05 Mar 2024
Published: 12 Mar 2024
J Short Name: AJSCCR

Citation:

Balodis A. Ewing Sarcoma of the Lumbar Spine With Lung Metastases in A 20-Year-Old Adult: A Rare Case Report. Ame J Surg Clin Case Rep. 2024; 7(13): 1-8

Keywords:

Case Report; Ewings Sarcoma; Magnetic Resonance Imaging; Lumbar Region

1. Abstract

1.1. Background: Ewing sarcoma (ES), a rare bone tumor primarily affecting adolescents and young adults, exhibits aggressive behavior, typically originating from bones or nearby soft tissues. Histopathology reveals a small round cell tumour, posing a challenge in distinguishing from small cell carcinoma, sarcomas, or lymphoma. This report outlines a 20-year-old man's case of lumbar spine ES with lung metastases.

1.2. Case Report: A 20-year-old male complained of back pain radiating to both legs, particularly the right. No signs of paralysis were evident. Magnetic Resonance Imaging revealed a lumbar mass with extradural spread in the spinal canal, compressing the dural sac and extending through the intervertebral foramen, auto necrosis areas were identified which led to working diagnosis of Schwannoma. The surgical extraction of the lumbar mass was performed. Immunohistochemical analysis of operative material revealed small round tumour cells with CD99 positivity. Subsequently, a t (11; 22) (q24.3; q12.2) translocation was identified, confirming the histopathological diagnosis of Ewing sarcoma. Two months post-surgery, lung metastases and hypermetabolism in L2 vertebra, spinal cord, and TH11-TH12 tissue were detected. The next step in the patient's treatment plan involves chemotherapy.

1.3. Conclusion: Ewing's sarcoma, a fast-growing malignancy, requires a multidisciplinary approach due to its clinical and radiographic features. This report underscores the challenge of distinguishing primary bone Ewing sarcoma from bone metastasis of other small round cell malignancies. The tumour's unusual location may complicate diagnosis, potentially leading to confusion with schwannoma. Early, precise diagnosis is crucial for prompt treatment.

2. Background

Ewing sarcoma (ES), known for its high aggressiveness and primarily found in children, is a bone and soft tissue tumor that typically arises from bones or the surrounding soft tissue. [1] ES reaches its peak incidence in adolescents aged 10-20 years, with an annual occurrence of 1-3 cases per 1,000,000. [2, 3] This disease is associated with male sex and the Caucasian race. [4, 5]. Ewing's sarcoma typically manifests within the central regions of the body and the elongated bones. [1, 2] Among the areas most frequently impacted by Ewing's sarcoma in the central skeletal structure are the pelvis, scapula, ribs, vertebral column, and clavicle. [2] In cases of Ewing's sarcoma affecting the elongated bones, the humerus, tibia, and forearm bones are the principal sites of involvement. [1, 2, 5] ES originating primarily in the spine is classified as an infrequent occurrence. [5, 6]. The Ewing's tumor family (EFT) includes Ewing sarcoma of bone (ESB), extraosseous Ewing sarcoma (EES), peripheral neuroectodermal tumor and Askin's tumor. ESB accounts for approximately 70% of the tumors in this family. [7] Patients with ES commonly present with pain and swelling, often reporting a history of trauma around the time of diagnosis, with symptoms persisting for more than 6 months before the initial medical visit; some may also exhibit systemic symptoms like fever or weight loss. [4, 5, 8] At the time of diagnosis, approximately 20% of patients exhibit metastatic disease, with over 20% of these

cases involving the lungs or pleura. [9] While systemic treatment has notably improved survival rates for patients with localized disease, those diagnosed with metastatic disease face a challenging prognosis, with less than 30% surviving beyond 5 years, and for recurrent cases, whether local or distant, the event-free 5-year survival probability drops to just 10%. [4, 5] This malignancy is highly aggressive. Radiological examination, including Magnetic Resonance Imaging (MRI) or Computed Tomography (CT) scans, is necessary to confirm the suspicion of ES. Radiologic examinations, such as CT scans or MRI, are also unable to generate distinct imaging for Ewing's sarcoma. [5, 6] In the absence of distinct identifying markers, distinguishing between various pathologies becomes a challenging task. Morphologically, Ewing's sarcoma is characterized as an undifferentiated small round blue-cell malignancy with low mitotic activity. [2]The differential diagnosis for small round cell tumors is extensive, encompassing entities such as Neuroblastoma, Rhabdomyosarcoma, Wilms Tumor, Lymphoma, Primitive Neuroectodermal Tumor (PNET), Synovial Sarcoma, Desmoplastic Small Round Cell Tumor (DSRCT) and many others. [3, 5, 10] Distinguishing Ewing sarcoma from other small blue cell tumors necessitates cytogenetic or immunohistochemical studies. [8] ES Tumors usually contain the surface antigen CD99 in over 95% of cases. [11, 12] Unfortunately, the CD-99 antigen is not entirely specific to Ewing's sarcoma, as it is also expressed in other types of primitive neuroectodermal tumors. [2, 8, 13] Furthermore, Ewing sarcomas typically exhibit periodic acid–Schiff (PAS) positivity due to intracellular glycogen and are negative for reticulin staining. [5] In contrast, lymphomas are PAS negative and reticulin positive, also exhibit positive staining for leukocyte common antigen, as well as other T- and B-cell antigens. [5] Embryonal rhabdomyosarcoma demonstrates positivity for desmin, myoglobin, and muscle-specific actins.[5] The translocation t (11; 22) (q24; q12) is highly prevalent in Ewing sarcoma [8], being detected in over 90% of cases. [2,5] Molecular genetic studies, incorporating fluorescence in situ hybridization (FISH) and/or reverse transcription-polymerase chain reaction (RT-PCR), are essential for making the definitive distinction. [8] Due to the nonspecific symptoms, accurately diagnosing Ewing's sarcoma remains a challenge that relies on a histological examination for a definitive diagnosis. [6] To gain a deeper insight into the diagnosis and treatment of Ewing sarcoma, we delve into pertinent case studies, such as the one by Ye et al., which examines the case of a 23-year-old man. Following initial primary sacral Ewing sarcoma, the individual developed metastases in the rib, lung, and multifocal skull subsequent to undergoing surgical intervention and a series of adjuvant therapies.[14] Our case report will present a rare case of ES occurring in the lumbar levels in a 20-year-old male. The primary tumor is localized in the lumbar region, with subsequent metastases spreading to the lungs and thoracic levels of the spine.

3. Case Report

The 20-year-old male patient was treated symptomatically when he first experienced back pain (summer 2022). The treatment was administered under the careful supervision of both a physiotherapist and a family doctor.

Over the span of six months, the patient's condition deteriorated, and by November 2022, they reported experiencing back pain that extended to both legs, with a notable emphasis on the right leg. It's worth noting that there were no signs of paresis accompanying the pain. Dysesthesia was observed in the right L2 dermatome. A lumbar Computed Tomography (CT) was previously conducted in an outpatient setting, revealing the presence of a lumbar mass. Subsequently, a Magnetic Resonance Imaging (MRI) was performed for diagnostic purposes, revealing a pathological mass/tumor (Craniocaudal (CC) 6, 3 cm x Anteropos-terior (AP) 6, 2 cm x Latero-lateral (LL) 4, 6 cm) located at the lumbar level. This mass exhibited extradural extension within the spinal canal. The mass/tumor was observed to compress the dural sac and extending beyond the spinal canal via the intervertebral fora-men. Regions of necrosis were identified, leading to a working diagnosis of Schwannoma (Figures 1, 2).

The patient was admitted to the hospital as part of a scheduled plan for the upcoming surgical procedure. The procedure involved a lumbotomy on the right side, with resection of mass at the L2 level and hemilaminectomy at the L1 and L2 levels (Figure 3). The pathological mass/tumor was successfully removed during the procedure.

A postoperative follow-up MRI in December 2022 indicates the presence of fluid at the surgical site. Significant edema is evident along the deep muscles, particularly on the right side of the psoas major muscle. There was fluid observed along the m.psoas, possibly with hemorrhagic components, that was pushing into the spinal canal, causing slight narrowing. However, there was no evidence of stenosis in this area. Among the postoperative alterations, there appears to be a minor remaining tissue within the foraminal region at levels TH12-L1 and L2-L3. Additionally, modifications are observed in the body and dorsal arch of the right-sided L2 vertebra, accompanied by bone sclerotic changes (Figure 4, 5).

Magnetic Resonance Diffusion-Weighted Imaging (MR DWI) sequence, edema was detected in the vertebral body, along with a pronounced suspicion of pathological infiltration of the vertebra (Figure 6).

Upon examination of the material extracted during the surgery, the tumor was stained with hematoxylin-eosin, revealing round-shaped and monomorphic cells with hyperchromic nuclei. The tumor was observed to have a papillary structure with pseudo-rose formations, where tumor cells were arranged around blood vessels, which is indicative of a small blue cell sarcoma (Figure 7). Immunohistochemical examination reveals diffuse, strongly positive

CD99, and proliferative index (Ki-67) 10-15 %. Negative results were observed for the following markers: Glial Fibrillary Acidic Protein (GFAP), S100, Epithelial Membrane Antigen (EMA), actin, CD56, desmin, chromogranin, synaptophysin, CKAE1/AE3, LCA, CD34, and CD138. After undergoing the FNCLCC grading system, the tumor was graded as Grade 1. The diagnosis was validated through fluorescence in situ hybridization (FISH), revealing the presence of the translocation t (11;22) (q24.3; q12.2) (EWS-R1::FLI1).

After being discharged from the hospital, the patient reported numbness in the anterior wall of the abdomen below the surgical incision, which decreased dynamically. From a neurological perspective, there were no indications of paresis, and the patient's tactile and deep sensations remained unaffected. The surgical incisions were healing well, exhibiting primary closure and devoid of any complications. The patient received a recommendation for chemotherapy and proton beam therapy, which unfortunately were not available. Two months after the surgery (February 2023) control thoracic CT showed multiple intrapulmonary nodules in the middle and lower subpleural fields of both lungs - most likely metastasis (Figure 8 and 9). Video-assisted thoracic surgery (VATS) marginal resection of the right middle lobe was performed in March 2023 and the material extracted during the surgery came back positive - metastatic sarcoma. To assess the potential for distant metastasis and postoperative developments, Fluorine-18 Fluorodeoxyglucose Positron Emission Tomography/Computed Tomography (18F [FDG] PET/CT) was conducted immediately after Video-Assisted Thoracoscopic Surgery (VATS). Another scan was performed three months later following prescribed guidelines. The results revealed subtle metabolic changes in specific spinal areas and the surgical site, possibly indicative of residual pathological tissue or reactive changes. Multiple lung metastases were identified without significant hypermetabolic activity, likely due to their small size. [12] (max 0, 6 cm diameter). In comparison with the previous postoperative control examination conducted in December 2022, the current MRI reveals the presence of foraminal and extraforaminal contrast agent collecting tissue at the Th12-L1 level. Furthermore, the MRI reveals the presence of dorsal infiltration in the Th12 vertebral body and infiltration in the L2 vertebral body (Figure 10). As of now, the patient has been tolerating the therapy well after initiating chemotherapy in March 2023, following the Vincristine, Doxorubicin (Adriamycin), Cyclophosphamide, Ifosfamide, and Etoposide (VDC-IE) protocol.

Figure 1: (A) Coronal T2-weighted magnetic resonance imaging (MRI) reveals a pathological tumor mass located on the right side of the L2-L3 lumbar level (arrow). This mass exhibits extradural spread within the spinal canal (arrowhead), resulting in compression of the dural sac. Furthermore, it extends beyond the spinal canal through the intervertebral foramen (star). **(B) Sagittal T2-weighted MRI** showing pathological tumor mass on the right side of L2-L3 lumbar level (arrow). Working diagnosis - Schwannoma.

Figure 2: Axial T2-weighted magnetic resonance imaging reveals compression of the dural sac (arrowhead). The pathological mass grows through m. psoas (arrow). The pathological formation affects the right kidney and pushes the pyelon and renal vessels ventrally (star).

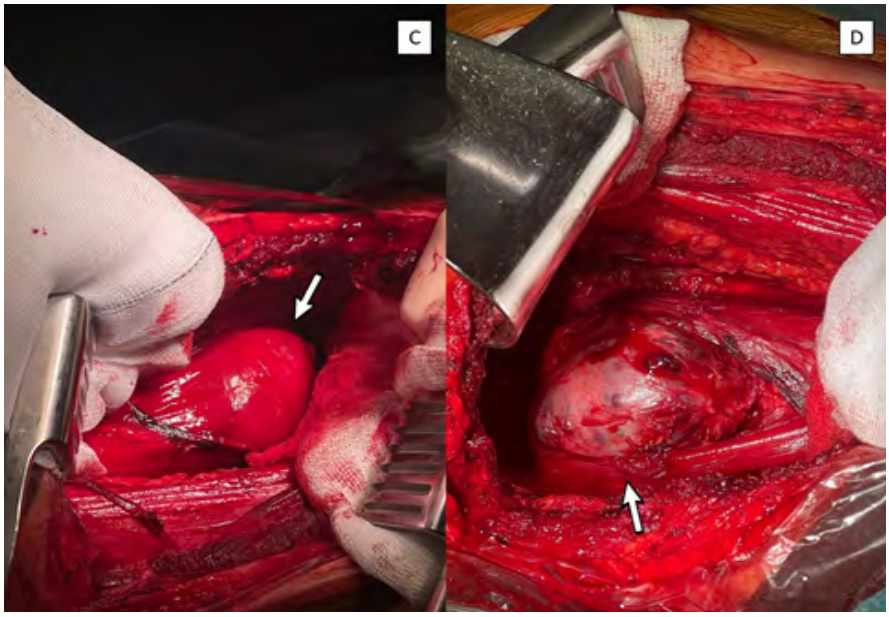

Figure 3: (C) Right lumbotomy, right L2 schwannoma's resection, and hemilaminectomy at the L1 and L2 levels. **(D)** Pathological tissue visualized from the right L2 root, the formation has completely overgrown and destroyed the right L2 root.

Figure 4: Postoperative Coronal T2-weighted magnetic resonance imaging (December 2022) illustrates the presence of fluid at the surgical site (Arrow), significant edema observed along the deep muscles and on the right side of the psoas major muscle. Despite a minor reduction in the width of the spinal canal, there is no discernible evidence of stenosis within this region (arrowhead).

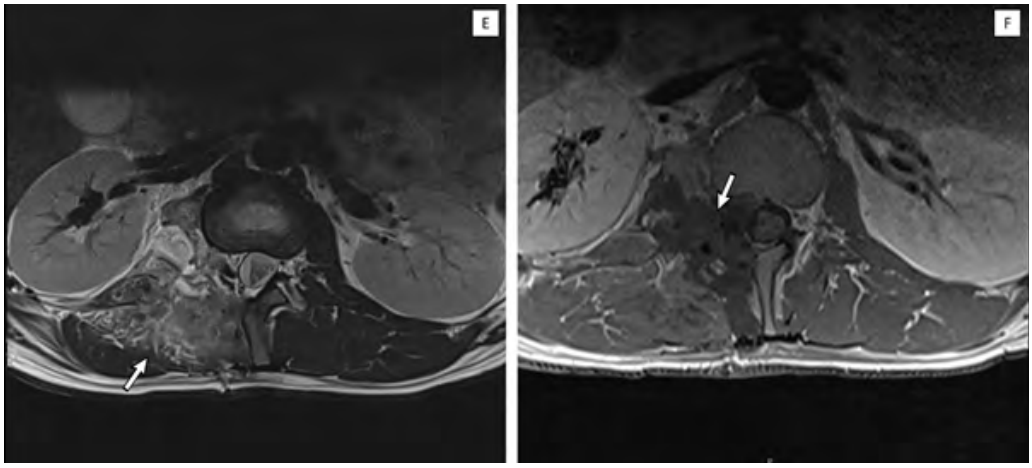

Figure 5: (E) Postoperative T2-weighted and (F) T1 - weighted magnetic resonance imaging reveals extensive edema along deep muscles and on the right side of psoas major muscle and fluid in the operation site (Arrows)**.**

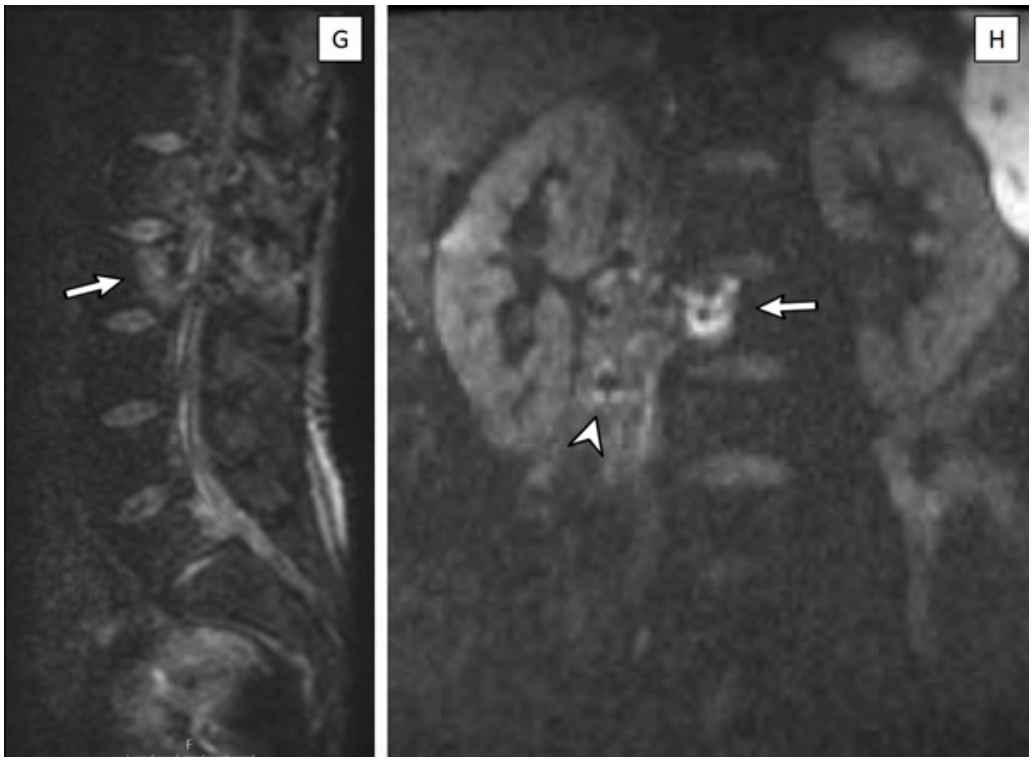

Figure 6: Postoperative follow-up (G) sagittal and (H) coronal Diffusion-Weighted Imaging magnetic resonance imaging show edema near the vertebral area (arrowhead) and a notable suspicion of pathological infiltration in the vertebra (Arrow).

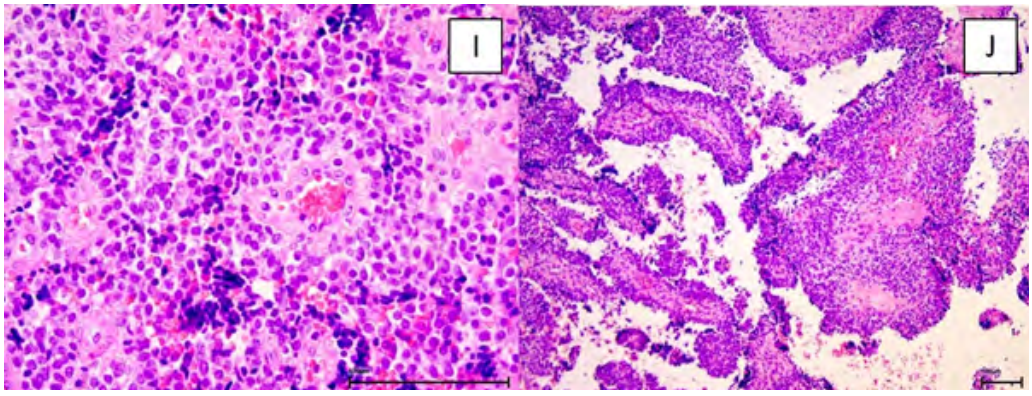

Figure 7: Hematoxylin and eosin staining (I) presents tumor material made of round-shaped, monomorphic cells with hyperchromatic nuclei. The tumor has pseudo-rosete structures. (J) Hematoxylin and eosin staining presents tumor material made of round-shaped, monomorphic cells with hyperchromatic nuclei. The tumor has a papillary structure.

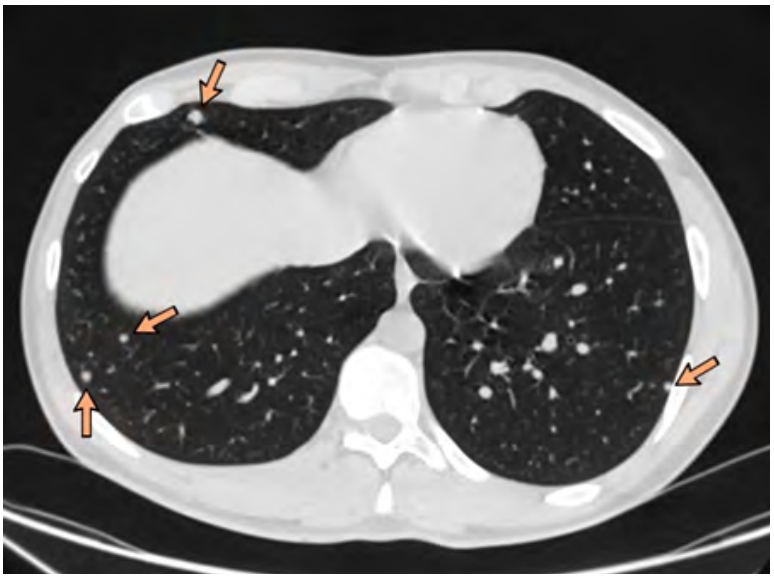

Figure 8: Control lung axial/oblique Computed Tomography demonstrates multiple intrapulmonary nodules in the middle and lower fields of both lungs and subpleural (arrows) - most likely metastatic disease.

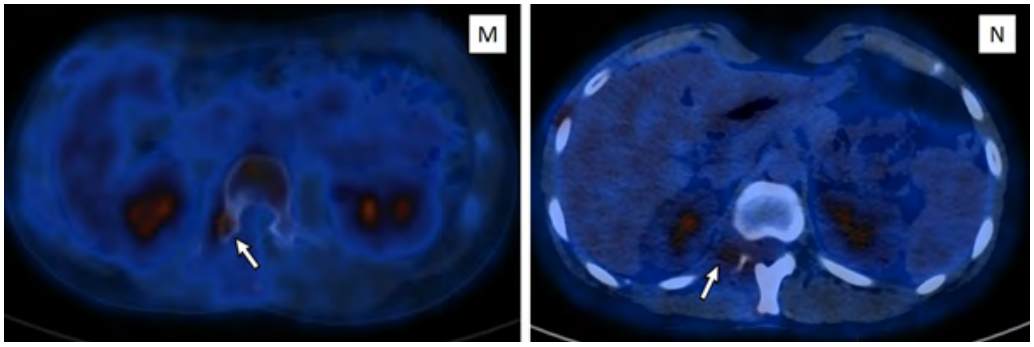

Figure 9: (M) [Fluorine-18] Fluorodeoxyglucose Positron Emission Tomography (PET) / Computed Tomography ([18F] FDG PET/CT) shows Mild hypermetabolic changes in the right lateral growth of the L2 vertebra (Arrow), which may correspond to residual pathological tissue or reactive changes. **(N) [18F] FDG PET/CT.** Right Video-Assisted Thoracoscopic Surgery (VATS) was performed with marginal resection, the pleural drain was evacuated. Hypermetabolic tissue is apparent in the middle lobe of the right lung and the subpleural space, which can also be traced beneath the skin, presumably due to surgical manipulation. These changes are considered non-specific and reactive following the manipulation. Despite the presence of lung metastases identified in the previous CT scan, PET/CT did not exhibit hypermetabolism in these metastases, which could potentially be attributed to their small size.

Figure 10: (K) T2 axial magnetic resonance imaging (MRI) In comparison with the previous postoperative control examination from December 2022 - currently at Th12 - L1 level, foraminal and extraforaminal contrast agent collecting tissue. (Arrow). **(L) T1 sagittal post-contrast** (Gadovist) **MRI** reveals pathological tissue in the spinal canal (star) and infiltration in the vertebral bodies TH12 (arrow) and L2 (arrowhead).

4. Discussion

Ewing's sarcoma is an extremely rare diagnosis with an incidence of 1-3 cases per million [2]. Ewing sarcoma primarily manifests during childhood, a period marked by active bone growth. It predominantly targets the metaphyseal plates of long bones, with the sacrum being the most frequent spinal site. While cases involving the non-sacral spine have been documented, they remain exceptionally rare. [15] Due to its diverse locations and rarity, particularly within the lumbar region, diagnosing primary Ewing's sarcoma of the vertebral column can present a considerable challenge. [16] Radiological examinations, including Magnetic Resonance Imaging or Computed Tomography scans, are indispensable for confirming suspicions of Ewing sarcoma. However, neither CT nor MRI scans yield distinct imaging for Ewing's sarcoma. Consequently, the absence of identifiable markers complicates the differentiation between various pathologies. Histologically, Ewing's sarcoma manifests as an undifferentiated small round blue-cell malignancy with low mitotic activity, adding to the complexity of its differential diagnosis. [2] Immunohistopathology and genetic evaluations are necessary to confirm the diagnosis due to the absence of specific clinical manifestations, laboratory markers, and distinctive radiological features associated with the disease. The rarity of Ewing's sarcoma occurring in the lumbar levels becomes evident upon comparing our case report with others. Additionally, the diagnostic approach for this pathology remains consistent, emphasizing immunohistopathology due to the non-specific nature of radiological findings. Moreover, the clinical manifestations of Ewing's sarcoma can vary significantly based on its location. In contrast to findings in alternative case re-ports, it's evident that the metastasis of Ewing's sarcoma to various locations, like the lungs and other bones, is a recurrent phenomenon. Despite these variations, patient management remains akin to our approach, involving surgical intervention and systematic chemotherapy. This case report provides valuable insights into the unique presentation, diagnostic challenges, and treatment considerations of Ewing's sarcoma at the lumbar levels. Our aim is to contribute to the existing medical literature and enhance the understanding and management of this rare condition.

5. Conclusion

Primary Ewing's sarcoma affecting the lumbar level presents as a rare primary ma-lignant bone tumor, often suspected in young individuals experiencing rapidly worsening lower back pain. Diagnosis relies on thorough imaging studies and is definitively confirmed through detailed histological analysis and genetic testing. This report underscores the intricate diagnostic challenges inherent in distinguishing primary Ewing sarcoma of the bone from bone metastases of other small round cell malignancies, a task further com-plicated in advanced cases, particularly those with suspected lung involvement. Early and precise diagnosis is vital to ensure that appropriate treatment is given as soon as possible.

References

1. Mousavi SR, Farrokhi MR, Eghbal K, Dehghanian A, Rezvani A, Ghaffarpasand F, et al. Metastatic Thoracic and Lumbar Intramedullary and Extramedullary Ewing's Sarcoma: A Rare Case Report and Literature Review. J. Int. Med. Res. 2022; 50.
2. Immunohistology of Pediatric Neoplasms – ClinicalKey.
3. Khan S, Abid Z, Haider G, Bukhari N, Zehra D, Hashmi M, et al. Incidence of Ewing's Sarcoma in Different Age Groups, Their Associated Features, and Its Correlation With Primary Care Interval. Cureus 2021; 13: e13986.
4. Hesla AC. Papakonstantinou, A.; Tsagkozis, P. Current Status of Management and Outcome for Patients with Ewing Sarcoma. Cancers 2021; 13.
5. Malignant Tumors of Bone – ClinicalKey.
6. Kamal AF, Cahayadi SD, Shihab RA, Ramang DS. A Challenging Diagnosis: Lesson from Case Series of Sacral Ewing Sarcoma. Int. J. Surg. Case Rep. 2022; 94: 107073.
7. Ewing Sarcoma - Symptoms, Causes, Treatment | NORD.
8. Durer S, Gasalberti DP, Shaikh H. Ewing Sarcoma. In StatPearls; StatPearls Publishing: Treasure Island (FL), 2024.
9. Ozaki T. Diagnosis and Treatment of Ewing Sarcoma of the Bone: A Review Article. J. Orthop. Sci. Off. J. Jpn. Orthop. Assoc. 2015; 20: 250–263.
10. Sharma S, Kamala R, Nair D, Ragavendra TR, Mhatre S, Sabharwal R, et al.. Round Cell Tumors: Classification and Immunohistochemistry. Indian J. Med. Paediatr. Oncol. Off. J. Indian Soc. Med. Paediatr. Oncol. 2017; 38: 349–353.
11. Immunohistology of Head and Neck Lesions – ClinicalKey.
12. Llombart-Bosch A, Machado I, Navarro S, Bertoni F, Bacchini P, Alberghini M, et al.. Histological Heterogeneity of Ewing's Sarcoma/PNET: An Immunohistochemical Analysis of 415 Genetically Confirmed Cases with Clinical Support. Virchows Arch. Int. J. Pathol. 2009; 455: 397–411.
13. Pasello M, Manara MC, Scotlandi, K. CD99 at the Crossroads of Physiology and Pathology. J. Cell Commun. Signal. 2018; 12: 55–68.
14. Sacral Ewing Sarcoma with Rib, Lung, and Multifocal Skull Metastases: A Rare Case Report and Review of Treatments.
15. Cherraqi A, Lemrabet A, Dokal ID, Lrhorfi N, Belghiti H, Allali N, et al. Primary Ewing's Sarcoma of the Spine: About a Case. Glob. Pediatr. Health 2022; 9.
16. Gu HL, Zeng SX, Chang YB, Lin Z, Zheng QJ, Zheng XQ, et al. Multidisciplinary Treatment Based on Surgery Leading to Long-Term Survival of a Patient with Multiple Asynchronous Rare Primary Malignant Neoplasms: A Case Report and Literature Review. Oncol. Lett. 2015; 9: 1135–1141.